Hindawi Publishing Corporation
International Journal of Photoenergy
Volume 2013, Article ID 812097, 7 pages
http://dx.doi.org/10.1155/2013/812097

Research Article

Enhanced Photocatalytic Activity of ZrO_2-SiO_2 Nanoparticles by Platinum Doping

Mohammad W. Kadi[1] and R. M. Mohamed[1,2,3]

[1] *Department of Chemistry, Faculty of Science, King Abdulaziz University, P.O. Box 80203, Jeddah 21589, Saudi Arabia*
[2] *Advanced Materials Department, Central Metallurgical R&D Institute, CMRDI, P.O. Box 87, Helwan, Cairo 11421, Egypt*
[3] *Center of Excellence in Environmental Studies, King Abdulaziz University, P.O. Box 80216, Jeddah 21589, Saudi Arabia*

Correspondence should be addressed to R. M. Mohamed; rmmohammed@kau.edu.sa

Received 9 January 2013; Revised 17 February 2013; Accepted 18 February 2013

Academic Editor: David Lee Phillips

ZrO_2-SiO_2 mixed oxides were prepared via the sol-gel method. Photo-assisted deposition was utilized for doping the prepared mixed oxide with 0.1, 0.2, 0.3, and 0.4 wt% of Pt. XRD spectra showed that doping did not result in the incorporation of Pt within the crystal structure of the material. UV-reflectance spectrometry showed that the band gap of ZrO_2-SiO_2 decreased from 3.04 eV to 2.48 eV with 0.4 wt% Pt doping. The results show a specific surface area increase of 20%. Enhanced photocatalysis of Pt/ZrO_2-SiO_2 was successfully tested on photo degradation of cyanide under illumination of visible light. 100% conversion was achieved within 20 min with 0.3 wt% of Pt doped ZrO_2-SiO_2.

1. Introduction

Remediation of hazardous pollutants in air, water, and soil is an important route in environmental cleanup. Photocatalysis is one of the most promising techniques that can be used efficiently to achieve high removal rates of pollutants. When radiation is shined on semiconductor nanoparticles, electron-hole pairs form. For these pairs to be formed incident radiation energy should be greater than the band gap of the semiconductor. Some of the produced electrons will reach the surface of the crystal triggering an oxidation-reduction reaction. This phenomenon is widely exploited by researchers in pollutant remediation and other beneficial reactions. Triggered by a charge carrier an active intermediate of organic pollutant on the surface of the catalyst will form, and then it undergoes fast reactions ultimately yielding water and carbon dioxide.

Particle size, band gap, surface area, life-time of the electron-hole pair, stability, and other physical and chemical properties determine the photocatalytic efficiency of the material [1]. Researchers explored various pathways to enhance the properties of catalysts towards a desired function. Altering the preparation method, oxide mixing, and doping are examples of such pathways [2–6].

An important issue in choosing a photocatalyst is its band gap width. For example, the band gap of TiO_2, the most popular photocatalyst, lies within the range 3.0–3.2 eV. TiO_2 has been subjected to numerous experimentation that includes mixing with semiconductors, doping with various metals, and various preparation methods in an effort to increase its catalytic activity and fine tune its band gap, surface area, and decrease charge carriers recombination possibility [7–9].

ZrO_2 possesses properties such as thermal stability, high specific surface area, and other optical and electrical properties that make it an attractive photocatalyst [10, 11]. ZrO_2 was used in the photocatalytic gas-phase oxidations of methanol and hexane [12]. H_2-yields up to 29% were achieved in the steam reforming reaction of bioethanol using Pt/ZrO_2 catalyst [13]. ZrO_2-SiO_2 mixed oxides exhibit yet bitter stability and photocatalytic efficiency [14, 15]. The effect of zirconia to silica ratio on methane reforming with CO_2 was reported with high efficiency [16]. Many studies in the literature report

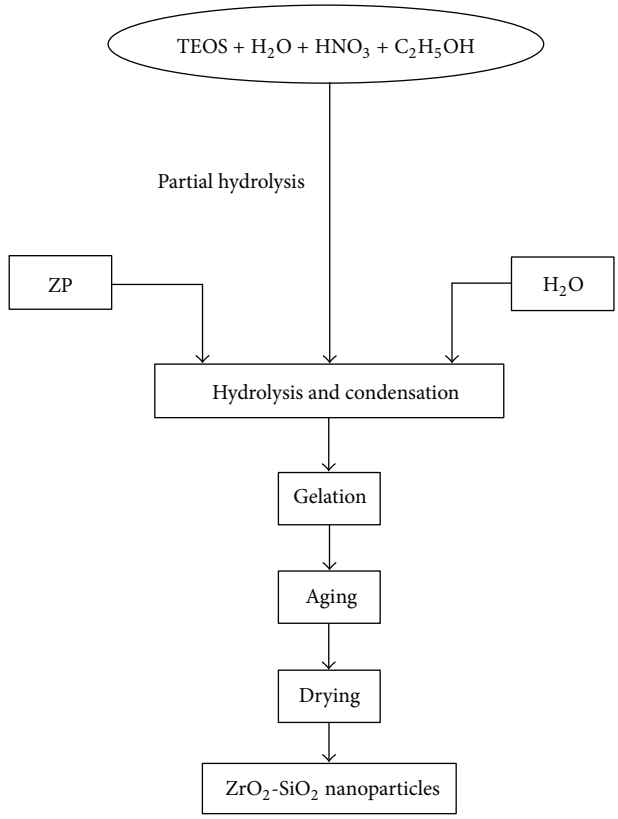

Figure 1: A schematic of ZrO_2-SiO_2 nanoparticles preparation.

temperature assisted catalytic reactions utilizing ZrO_2-SiO_2 [17, 18]. A photocatalytic application of Pt doped ZrO_2-SiO_2 using a visible-range light source has not been reported. Visible range illumination would increase the photocatalytic efficiency of the reaction if the photocatalyst is to be used in direct sunlight as visible light constitute about 40% of the total emitted energy of the sun [19]. For a catalyst to be able to excite on illumination with natural sunlight the band gap should be tuned down to visible range wavelengths. In this work we report improved catalyst characteristics resulting from room temperature sol-gel preparation of ZrO_2-SiO_2 and Pt doped ZrO_2-SiO_2. Enhanced photocatalysis using visible irradiation is reported as a direct effect of Pt doping. Optimum conditions for enhanced photocatalysis of CN^- are presented.

2. Experimental

2.1. Materials. Tetraethylorthosilicate $Si(OC_2H_5)_4$ (TEOS) 98% (Acros), Zirconium(IV) propoxide 70 wt% solution in 1-propanol $Zr(OCH_2CH_2CH_3)$ (ZP) (Aldrich), and Chloroplatinic acid H_2PtCl_6 (Sigma-Aldrich) were used as sources of Si, Zr, and Pt, respectively. Absolute Ethanol (Aldrich), Nitric acid HNO_3 (Aldrich), and deionized water were used in the preparation of metal oxides. All chemicals were used as received without further purification.

2.2. Preparation of ZrO_2-SiO_2 Nanoparticles. In the sol-gel preparation of ZrO_2-SiO_2 nanoparticles with 30 : 70 molar ratio, 20 mL of TEOS was mixed with ethanol, deionized water, and HNO_3 with magnetic stirring for 60 min. A calculated amount of $Zr(OCH_2CH_2CH_3)$ and deionized water were then added simultaneously in a drop wise fashion to the Si sol. After continuous stirring for another 60 min, the prepared sol was left to stand until the formation of gel. The gel was then calcined at 550°C for 5 h in air to obtain the ZrO_2-SiO_2 xerogel. A schematic representation of the preparation process is presented in Figure 1.

2.3. Platinum Doping. Platinum was deposited on the ZrO_2-SiO_2 particles via the photo-assisted deposition (PAD) route. In this procedure 0.1, 0.2, 0.3, and 0.4 wt% of Pt metal was deposited on ZrO_2-SiO_2 nanoparticles. PAD was achieved when UV-light was shined on a solution containing the ZrO_2-SiO_2 particles and the Pt metal source, an aqueous solution of H_2PtCl_6. Solutions were dried at 105°C. A 2 h H_2-reduction process (20 mL min^{-1}) at 400°C was enough to get the PAD-Pt/ZrO_2-SiO_2 particles.

2.4. Characterization. The specific surface area of the prepared samples was evaluated from the adsorption-desorption isotherms of nitrogen at −196°C detected using a Nova 2000 series apparatus (Chromatech). The specific surface

areas of materials were calculated using the BET method applying the Brunauer-Emmett-Teller (BET) equation. Prior to measurements all samples were degassed under vacuum at 200°C for 2 h.

Particle size was determined from X-ray diffraction (XRD) analysis carried out at room temperature using a Bruker axis D8 instrument using Cu Kα radiation (λ = 1.540 Å). The crystallite size of ZrO_2-SiO_2 and PAD-Pt/ZrO_2-SiO_2 particles was calculated using Scherer equation

$$d = \frac{B\lambda}{\beta_{1/2}\cos\theta}, \quad (1)$$

where d is the average particle size of the material under investigation, B is the Scherer constant (0.89), λ is wavelength of the X-ray beam, $\beta_{1/2}$ is the full width at half maximum of the diffraction peak, and θ is the diffraction angle [20].

Surface morphology of all prepared catalysts was examined using scanning Electron microscope (JEOL 5410 Japan) and transmission electron microscope (JEOL-JEM-1230). Before the prepared catalysts loading into the TEM, they were suspended in ethanol, followed by ultra-sonication for 30 min.

Band gap energies of the samples were determined by UV-Visible diffuse reflectance spectra (UV-Vis-DRS) in air at room temperature in the wavelength range of 200–800 nm using UV/Vis/NIR spectrophotometer (V-570, JASCO, Japan). The band gap energies were calculated employing the equation:

$$E_g = \frac{1239.8}{\lambda}, \quad (2)$$

where E_g is the band gap (eV) and λ is the wavelength of the absorption edges in the spectrum (nm).

2.5. Photocatalytic Experiment. The application of the synthesized nanoparticles for the photodegradation of cyanide was investigated under visible light. Experiments were carried out using a horizontal cylinder annular batch reactor. The photocatalyst was irradiated with a blue fluorescent lamp (150 W, maximum energy at 450 nm) doubly covered with a UV cut filter. The intensity data of UV light is confirmed to be under the detection limit (0.1 mW/cm^2) of a UV radiometer.

In a typical experiment, a desired weight of the catalyst was suspended into a 300 mL, 100 mg/L potassium cyanide (KCN) solution. Ammonia solution was used to set the pH of the experiment at 10.5 to avoid evolution of HCN gas. The reaction was carried out isothermally at 25°C and samples of the reaction mixture were analyzed at different time intervals for a total reaction time of one hour.

The CN^- concentration in samples was estimated by volumetric titration with $AgNO_3$, using potassium iodide to determine the titration end-point [21]. The removal efficiency of CN^- was measured by applying the following equation:

$$\%\text{Removal efficiency} = \frac{(C_0 - C)}{C_0} \times 100, \quad (3)$$

where C_0 is the initial concentration of the uncomplexed CN^- in the solution and C is the concentration of unoxidized CN^- in the solution.

Table 1: The particle size, band gap, and surface area of the prepared catalysts.

Sample	Particle size, nm	Band gap, eV	Surface area, m^2/g
ZrO_2-SiO_2	15.3	3.04	418
0.1 Pt/ZrO_2-SiO_2	14.7	2.88	397
0.2 Pt/ZrO_2-SiO_2	14.0	2.73	363
0.3 Pt/ZrO_2-SiO_2	13.7	2.61	354
0.4 Pt/ZrO_2-SiO_2	13.3	2.48	347

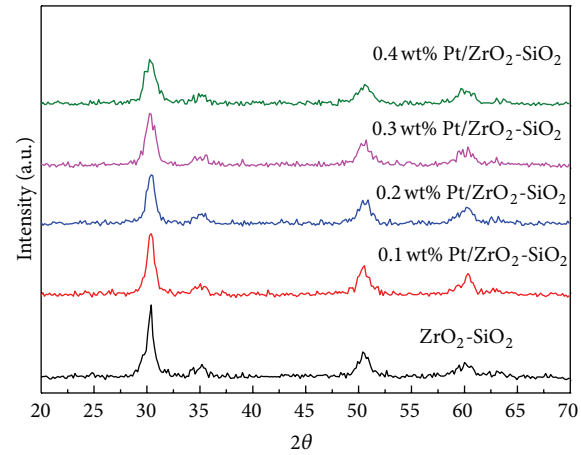

Figure 2: XRD patterns of pure and Pt doped ZrO_2-SiO_2.

3. Results and Discussion

3.1. Textural Properties. XRD patterns of each parent ZrO_2-SiO_2 and Pt/ZrO_2-SiO_2 nanoparticles prepared by PAD method are compared in Figure 2. XRD patterns show that the structural characteristics of the prepared ZrO_2-SiO_2 and Pt/ZrO_2-SiO_2 compare perfectly to ZrO_2 (JCPDS: 88-1007). This indicates that ZrO_2 structure was preserved after the application of the photo-assisted deposition (PAD) method. No diffraction peaks of Pt in the patterns of Pt/ZrO_2-SiO_2 samples were observed. This is probably attributed to the low Pt doping content. Moreover, the data may imply that Pt is well dispersed within the ZrO_2-SiO_2 phase. Pt played a prominent role in the process of crystallization as can be seen from XRD patterns showing that the ZrO_2 phase characteristic diffraction peaks became broad and the diffraction peaks' intensity decreased with increased Pt loading. Calculated crystallize size from XRD measurements (Table 1) shows decreased crystallize size with the increase in doping percentage. The crystallize size decreased from 15.3 nm for ZrO_2-SiO_2 to 13.3 nm for 0.4 Pt/ZrO_2-SiO_2.

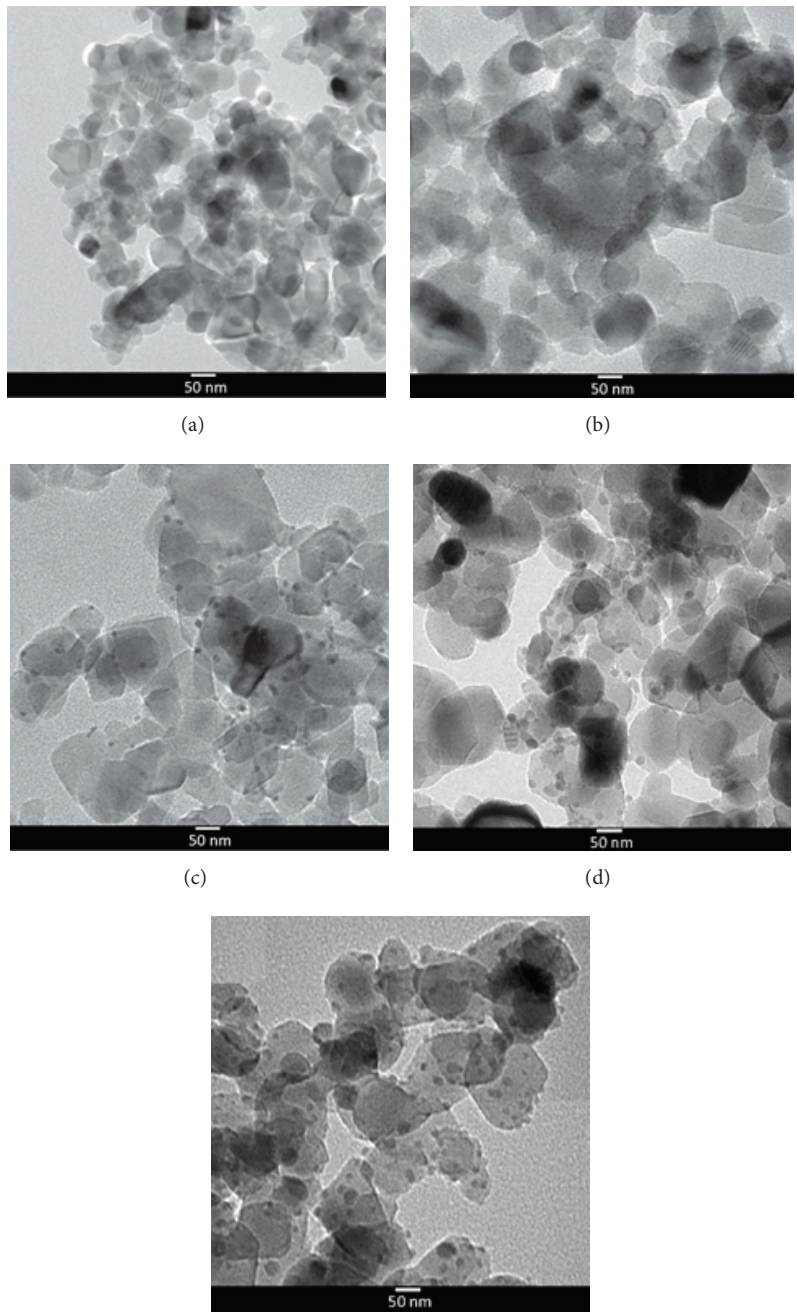

Figure 3: TEM images of ZrO_2-SiO_2 (a), 0.1 Pt/ZrO_2-SiO_2 (b), 0.2 Pt/ZrO_2-SiO_2 (c), 0.3 Pt/ZrO_2-SiO_2(d), and 0.4 Pt /ZrO_2-SiO_2 (e).

TEM images of Pt/ZrO_2-SiO_2 nanoparticles prepared by the PAD method are shown in Figure 3. The figure reveals that Pt ion is dispersed on the surface of the catalyst. The diameter of the dispersed Pt ions increases with the increase in wt% of Pt.

3.2. Surface Area Analysis. Specific surface area (S_{BET}) of parent ZrO_2-SiO_2 and Pt/ZrO_2-SiO_2 nanoparticles was determined. The S_{BET} values were 418, 397, 363, 354, and 347 m^2/g for the ZrO_2-SiO_2, 0.1 Pt/ZrO_2-SiO_2, 0.2 Pt/ZrO_2-SiO_2, 0.3 Pt/ZrO_2-SiO_2,and 0.4 Pt/ZrO_2-SiO_2, respectively, revealing a mild decrease in surface area with increased Pt doping.

3.3. Optical Characterization. The UV-Vis diffuse reflectance spectra of the ZrO_2-SiO_2 and Pt/ZrO_2-SiO_2 nanoparticles are displayed in Figure 4. The loading of Pt ions into the ZrO_2-SiO_2 caused a red shift toward a higher wavelength from 430 to 500 nm for different loadings of Pt compared to a wavelength of about 410 nm for the undoped ZrO_2-SiO_2. The direct band gap energies for the ZrO_2-SiO_2 and

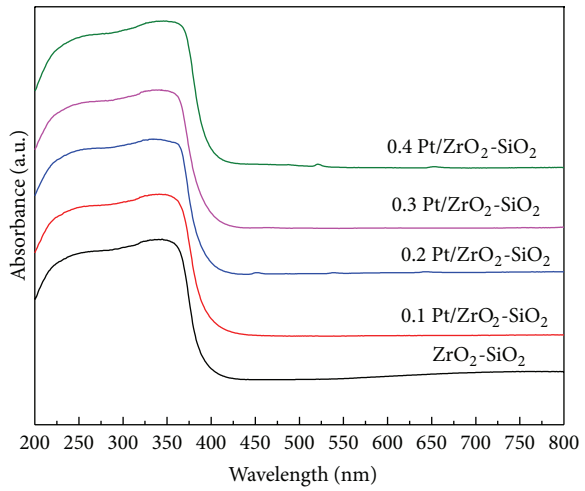

Figure 4: UV-Vis absorption spectra of ZrO_2-SiO_2 and various combinations of Pt/ZrO_2-SiO_2.

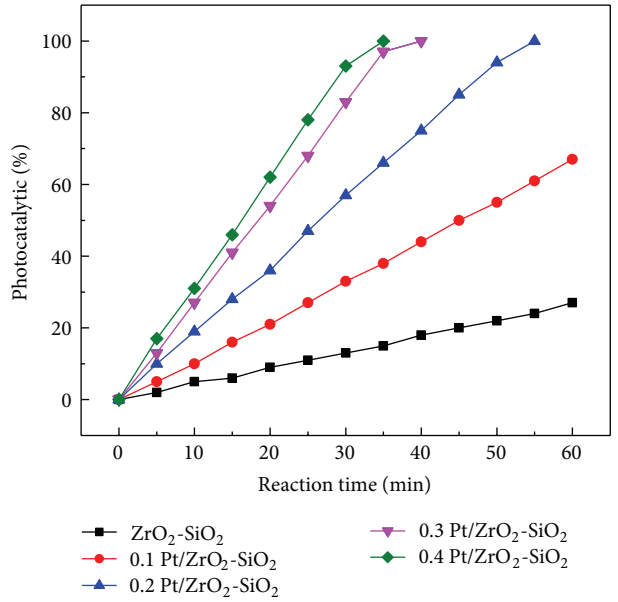

Figure 5: The effect of wt% of Pt on photocatalytic degradation % of CN^- with ZrO_2-SiO_2 and various combinations of Pt/ZrO_2-SiO_2.

Pt/ZrO_2-SiO_2 calculated from their reflection spectra based on a method suggested by Kumar et al., Korosi et al., and Yao et al. [22–24] are tabulated in Table 1. It is clear that the energy gap decreased with the increase in the Pt ions wt%.

It is generally accepted that the incorporation of noble metal nanoparticles into the semiconductor-based catalysts could enhance the light absorption of catalyst in the visible-light region. This led to a shift of the absorption edge toward longer wavelength, indicating a decrease in the band gap energy and that more photogenerated electrons and holes could participate in the photocatalytic reactions. In case of Pt as a noble metal, Pt seems to modify the interface of ZrO_2-SiO_2 in a way that altering the mechanism that photogenerated charge carriers undergo recombination or surface reactions. This would force ZrO_2-SiO_2 mixed oxide to be activated in the visible region. The shift in emission position could be attributed to the charge transfer between the Pt generated band and the conduction band of ZrO_2-SiO_2 as a semiconductor. This decrease in the bad gap energy will result in an increased photocatalytic efficiency that overcomes the effect of the decrease in the surface area caused by Pt doping.

3.4. Photocatalytic Activities. The photocatalytic activity is known to be dependent on the crystallinity, surface area, and morphology and it may be improved by slowing the recombination of photogenerated electron-hole pairs, extending the excitation wavelength to a lower energy range, and increasing the amount of surface-adsorbed reactant species. In general, the process for photocatalysis begins when supra-band gap photons are directly absorbed consequently generating electron-hole pairs in the semiconductor particles. This is followed by diffusion of the charge carriers to the surface of the particle where the interaction with water molecules would produce highly reactive species of peroxide (O_2^-) and hydroxyl radical ($OH^\bullet$) responsible for the degradation of adsorbed organic molecules. Step-reactions in the photocatalytic process leading to the degradation of CN^- are presented in the following sequence:

$$\begin{aligned}
ZrO_2 + h\nu &\longrightarrow e^- + h^+ \\
e^- (Pt) &\longrightarrow e_{tr}^- (Pt) \\
e_{tr}^- + O_2 (ads) &\longrightarrow O_2^- \\
2e_{tr}^- + 2H^+ + O_2 &\longrightarrow H_2O_2 \\
H_2O_2 + e_{tr}^- &\longrightarrow OH^- + OH^\bullet \\
h^+ + H_2O &\longrightarrow H^+ + OH^\bullet \\
2CN^- + 4OH^\bullet &\longrightarrow 2N_2 + 2CO_2 + 2H_2
\end{aligned} \tag{4}$$

In the prepared Pt/ZrO_2-SiO_2 enhancement of the photocatalytic activity of the catalyst is realized through two mechanisms. The first being prevention of the recombination of the electron-hole pair by Pt atoms in the Pt/ZrO_2-SiO_2 catalyst. Doped metal atoms on a semiconductor often act as electron traps [1]. The second reason for the improved photocatalytic activity is the reduced band gap energy that allows absorption of photons in the visible range.

Figure 5 shows the photocatalytic degradation of cyanide solution with ZrO_2-SiO_2 catalyst with different wt% of Pt upon visible light illumination under the following conditions: pH = 10.5, 300 mL of 100 ppm KCN, and 0.20 g of catalyst. The figure indicates that the photocatalytic efficiency of pure ZrO_2-SiO_2 does not exceed 30% after one hour reaction time. The low efficiency of the catalyst in an experiment where a visible light is shined on the catalyst-KCN solution is explained by the wide band gap of the catalyst. As

Table 2: Observed rate constants of CN^- degradation using ZrO_2-SiO_2 and Pt/ZrO_2-SiO.

Sample	$k \times 10^{-4}$, min^{-1}
ZrO_2-SiO_2	20
0.1 Pt/ZrO_2-SiO_2	50
0.2 Pt/ZrO_2-SiO_2	110
0.3 Pt/ZrO_2-SiO_2	200
0.4 Pt/ZrO_2-SiO_2	220

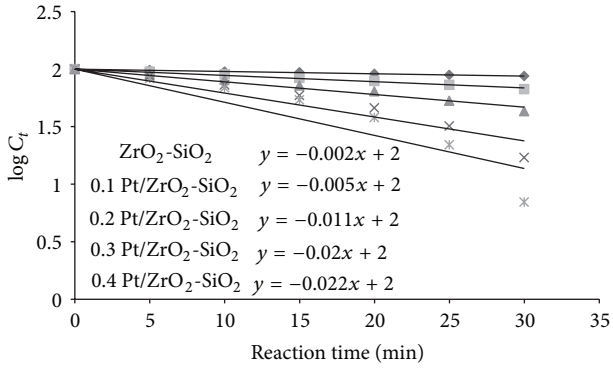

Figure 6: The effect of wt% of Pt on the rate constant of CN^- with ZrO_2-SiO_2 and various combinations of Pt/ZrO_2-SiO_2.

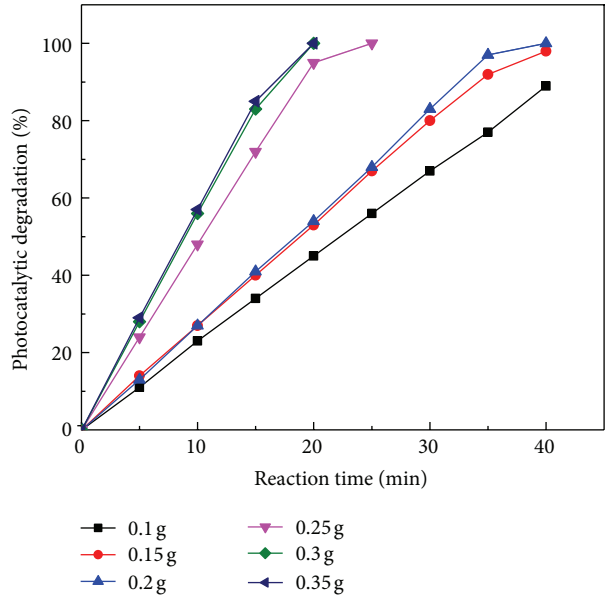

Figure 7: The effect of loading of 0.3 wt% Pt/ZrO_2-SiO_2 on CN^- degradation.

the band gap decreases with the increased doping wt% of Pt the efficiency of the photodegradation increases sharply along with rapid decrease in time needed for complete reaction. Looking at Figure 5 again, one can choose 0.3 wt% Pt/ZrO_2-SiO_2 as optimum combination for it contains enough Pt to achieve 100% degradation in less than 40 min.

Table 3: Observed rate constants of CN^- degradation using different loadings of 0.3 wt% Pt/ZrO_2-SiO_2.

Sample	$k \times 10^{-4}$, min^{-1}
0.10	110
0.15	140
0.20	200
0.25	330
0.30	450
0.35	470

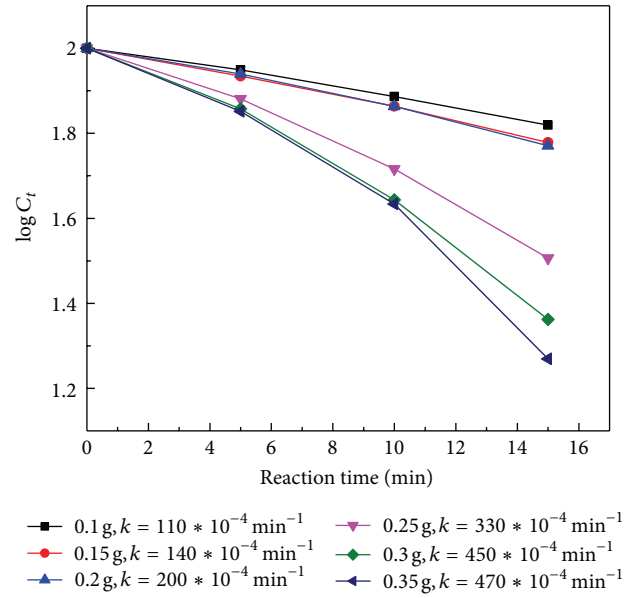

Figure 8: The effect of loading of 0.3 wt% Pt/ZrO_2-SiO_2 on the rate constant of CN^- degradation.

The reaction order with respect to cyanide concentration was determined by plotting reaction time versus log[cyanide] according to (Figure 6)

$$\log [C]_t = -kt + \log [C]_0, \quad (5)$$

where $[C]_0$ and $[C]_t$ represent the concentration of the substrate in solution after illumination at 0 and t min, respectively, and k is the apparent rate constant (min^{-1}).

The apparent rate constants are summarized in Table 2. The results show that the reaction followed first-order kinetics. The rate constants were found to be in the range of 20×10^{-4}–220×10^{-4} min^{-1}. The effect of different catalyst loading weights on the photocatalytic degradation of cyanide is shown in Figure 7. The graph shows that the increase in loading of the catalyst from 0.1 to 0.20 g increases cyanide removal efficiency from 89% to 100% after 40 min reaction time, respectively. Further increase in catalyst loading from 0.2 to 0.3 g decreases the reaction time from 40 to 20 min. No significant effect on cyanide removal efficiency and reaction time is observed with catalyst loading above 0.3 g. Therefore, the optimum condition for loading of catalyst is 0.30 g.

Plots of the reaction time versus log $[C]_t$ (Figure 8) reveal a first-order kinetics with a range of rate constants 110×10^{-4} to 470×10^{-4} min^{-1} (Table 3).

4. Conclusions

Pt doping enhances the photocatalytic activity of ZrO_2-SiO_2 considerably. The sol-gel prepared Pt/ZrO_2-SiO_2 exhibits superb activity compared to the undoped ZrO_2-SiO_2. Optimization of reaction conditions leads to a conclusion that a 0.3 wt% of Pt doping and a use of 0.3 g of the catalyst on a 300 mL, 100 mg/L KCN solution yield 100% degradation of the CN^- species within 20 min irradiation of visible light.

References

[1] R. M. Mohamed, D. L. McKinney, and W. M. Sigmund, "Enhanced nanocatalysts," *Materials Science & Engineering*, vol. 73, no. 1, pp. 1–13, 2012.

[2] M. Yuan, J. Zhang, S. Yan et al., "Effect of Nd_2O_3 addition on the surface phase of TiO_2 and photocatalytic activity studied by UV Raman spectroscopy," *Journal of Alloys and Compounds*, vol. 509, no. 21, pp. 6227–6235, 2011.

[3] N. Yao, S. Cao, and K. L. Yeung, "Mesoporous TiO_2-SiO_2 aerogels with hierarchal pore structures," *Microporous and Mesoporous Materials*, vol. 117, no. 3, pp. 570–579, 2009.

[4] H. Tel, Y. Altas, M. Eral, S. Sert, B. Cetinkaya, and S. Inan, "Preparation of ZrO_2 and ZrO_2-TiO_2 microspheres by the sol-gel method and an experimental design approach to their strontium adsorption behaviours," *Chemical Engineering Journal*, vol. 161, no. 1-2, pp. 151–160, 2010.

[5] S. Yamazaki, Y. Fujiwara, S. Yabuno, K. Adachi, and K. Honda, "Synthesis of porous platinum-ion-doped titanium dioxide and the photocatalytic degradation of 4-chlorophenol under visible light irradiation," *Applied Catalysis B*, vol. 121-122, pp. 148–153, 2012.

[6] C. Karunakaran, R. Dhanalakshm, and P. Gomathisankar, "Phenol-photodegradation on ZrO_2. Enhancement by semiconductors," *Spectrochimica Acta Part A*, vol. 92, pp. 201–206, 2012.

[7] D. Nassoko, L. Yan-Fang, H. Wang, L. Jia-Lin, L. Yuan-Zhi, and Y. Yu, "Nitrogen-doped TiO_2 nanoparticles by using EDTA as nitrogen source and soft template: simple preparation, mesoporous structure, and photocatalytic activity under visible light," *Journal of Alloys and Compounds*, vol. 540, pp. 228–245, 2012.

[8] T. K. Ghorai, M. Chakraborty, and P. Pramanik, "Photocatalytic performance of nano-photocatalyst from TiO_2 and Fe_2O_3 by mechanochemical synthesis," *Journal of Alloys and Compounds*, vol. 509, no. 32, pp. 8158–8164, 2011.

[9] U. I. Gaya and A. H. Abdullah, "Heterogeneous photocatalytic degradation of organic contaminants over titanium dioxide: a review of fundamentals, progress and problems," *Journal of Photochemistry and Photobiology C*, vol. 9, no. 1, pp. 1–12, 2008.

[10] C. Karunakaran and S. Senthilvelan, "Photocatalysis with ZrO_2: oxidation of aniline," *Journal of Molecular Catalysis A*, vol. 233, no. 1-2, pp. 1–8, 2005.

[11] H. R. Pouretedal, Z. Tofangsazi, and M. H. Keshavarz, "Photocatalytic activity of mixture of ZrO_2/SnO_2, ZrO_2/CeO_2 and SnO_2/CeO_2 nanoparticles," *Journal of Alloys and Compounds*, vol. 513, pp. 359–364, 2012.

[12] C. Wu, X. Zhao, Y. Ren et al., "Gas-phase photo-oxidations of organic compounds over different forms of zirconia," *Journal of Molecular Catalysis A*, vol. 229, no. 1-2, pp. 233–239, 2005.

[13] T. Yamazaki, N. Kikuchi, M. Katoh et al., "Behavior of steam reforming reaction for bio-ethanol over Pt/ZrO_2 catalysts," *Applied Catalysis B*, vol. 99, no. 1-2, pp. 81–88, 2010.

[14] Z. Zhan and H. C. Zeng, "A catalyst-free approach for sol-gel synthesis of highly mixed ZrO_2-SiO_2 oxides," *Journal of Non-Crystalline Solids*, vol. 243, no. 1, pp. 26–38, 1999.

[15] H. Yoshida, M. G. Chaskar, Y. Kato, and T. Hattori, "Active sites on silica-supported zirconium oxide for photoinduced direct methane conversion and photoluminescence," *Journal of Photochemistry and Photobiology A*, vol. 160, no. 1-2, pp. 47–53, 2003.

[16] G. K. Reddya, S. Loridanta, A. Takahashia, P. Delichèrea, and B. M. Reddy, "Reforming of methane with carbon dioxide over Pt/ZrO_2/SiO_2 catalysts-Effect of zirconia to silica ratio," *Applied Catalysis A*, vol. 389, pp. 92–100, 2010.

[17] E. Kauppi, E. Rönkkönen, S. Airaksinen, S. Rasmussen, M. Banares, and A. Krause, "Influence of H_2S on ZrO_2-based gasification gas clean-up catalysts: MeOH temperature-programmed reaction study," *Applied Catalysis B*, vol. 111-112, pp. 605–613, 2012.

[18] R. Gomez, F. Tzompantzi, T. Lopez, and O. Novaro, "ZrO_2-SiO_2 mixed oxides as supports for platinum catalysts," *Reaction Kinetics & Catalysis Letters*, vol. 53, no. 2, pp. 245–251, 1994.

[19] A. L. Linsebigler, G. Lu, and J. T. Yates, "Photocatalysis on TiO_2 surfaces: principles, mechanisms, and selected results," *Chemical Reviews*, vol. 95, no. 3, pp. 735–758, 1995.

[20] P. Tyagi and A. G. Vedeshwar, "Grain size dependent optical band gap of CdI_2 films," *Bulletin of Materials Science*, vol. 24, pp. 297–300, 2001.

[21] A. I. Vogel, *Quantitative Inorganic Analysis*, Longmans, London, UK, 1978.

[22] V. Kumar, S. K. Sharma, T. P. Sharma, and V. Singh, "Band gap determination in thick films from reflectance measurements," *Optical Materials*, vol. 12, pp. 115–119, 1999.

[23] L. Korosi and I. Dekany, "Preparation and investigation of structural and photocatalytic properties of phosphate modified titanium dioxide," *Colloids and Surfaces A*, vol. 280, no. 146, 154 pages, 2006.

[24] S. Yao, X. Jia, L. Jiao, C. Zhu, and Z. Shi, "La-doped TiO_2 hollow fibers and their photocatalytic activity under UV and visible light," *Indian Journal of Chemistry A*, vol. 51, pp. 1049–1056, 2012.